Prion Protein Interaction with the C-Terminal SH3 Domain of Grb2 Studied Using NMR and Optical Spectroscopy†

Dominikus A. Lysek and Kurt Wüthrich*

Institut für Molekularbiologie und Biophysik, Eidgenössische Technische Hochschule Zürich, CH-8093 Zürich, Switzerland

Received March 16, 2004; Revised Manuscript Received June 7, 2004

ABSTRACT: Transmissible spongiform encephalopathies have been observed exclusively in organisms expressing the host-encoded prion protein (PrP). The function of the cellular isoform of PrP found in healthy organisms has so far not been identified, although there are indications of a role in signal transduction in neurons. To gain further insight into the functional properties of cellular PrP, this paper investigated the binding of the C-terminal SH3 domain of the murine growth factor receptor-bound protein 2 (Grb2) to the murine PrP, using NMR, fluorescence, and circular dichroism spectroscopy. The SH3-binding site in murine PrP was thus found to be in the highly conserved region of residues 100−109, which contains prolines in positions 101 and 104. The protein−protein interaction, with a K_D value of 5.5 μM, is abolished when either of these two prolines is replaced by leucine. In humans, two corresponding Pro → Leu exchanges are found in patients who present with the Gerstmann−Sträussler−Scheinker syndrome. The results of the present study thus indicate a possible mechanism by which amino acid exchanges could influence a specific protein−protein interaction in a complex signal transduction cascade, which might be of functional significance in health and disease.

Transmissible spongiform encephalopathies (TSE)[1] are fatal neurodegenerative diseases in man and other mammalian species, which are transmissible both in nature and in the laboratory (*1*). In these neuronal disorders, an aggregated isoform ("scrapie isoform", PrP^{Sc}) of the prion protein (PrP) is accumulated primarily in the brain. When compared with the solution structures available for the "cellular form" found in healthy organisms (PrP^{C}) (*2*−*5*), cryoelectron microscopy pictures of PrP^{Sc} (*6*) indicate that an important difference between the three-dimensional structures of PrP^{C} and PrP^{Sc} is located in the segment of residues 90−120 preceding the C-terminal globular domain. This polypeptide segment, which is flexibly disordered in PrP^{C} (*7*), seems to account at least in part for the significantly increased β-sheet content in PrP^{Sc} amyloid fibrils, when compared to PrP^{C} (*6*, *8*).

Through transgenic mouse experiments it has been shown that expression of the host prion protein is required for the onset of a TSE, which has never been observed in *Prnp*$^{0/0}$ mice (*9*). In contrast to this clear-cut implication of an important role of PrP^{C} for the susceptibility of mammalian organisms to outbreak of TSEs, the physiological role of PrP^{C} in healthy organisms remains unknown, although PrP is highly conserved among mammals and other higher animals (*10*, *11*). Thereby, a segment of about 25 amino acid residues (113−137 in mPrP) is particularly highly conserved. The first 12 residues of this segment are part of the flexible tail of PrP^{C}, and the remainder is incorporated in the globular domain.

Evidence has been published that PrP^{C} might have a role in signal transduction, and in particular it has been suggested that PrP^{C} might be important in neuronal cell differentiation (*12*) and that it has a downstream effect on the phosphorylation of the tyrosine kinase Fyn (*13*). Spielhaupter and Schätzl (*14*) showed through a yeast two-hybrid assay that PrP^{C} binds to the growth factor receptor-bound protein 2 (Grb2), which is a highly abundant, well-characterized adaptor protein in neurons. The PrP^{C} interaction site of Grb2 was then further shown to be in the C-terminal SH3 domain ("Src homology domain 3") of Grb2 (Grb2_cSH3).

Grb2 is a signaling molecule mostly known through its involvement in the Sos/Ras signaling cascade, which is critical for the control of cell proliferation and differentiation (*15*, *16*). Since its discovery, many additional protein interaction partners have been found (*17*), including the Wiskott−Aldrich syndrome protein (WASP), which plays a role in cytoskeletal regulation. Grb2 is made up of a central SH2 domain flanked by two SH3 domains. The binding interactions with partner proteins have been extensively investigated (*18*−*20*). Similar to all other SH3 domains, Grb2_cSH3 binds its ligands in a polyproline II (PPII) helix conformation, with a binding strength in the range of K_D = 1−100 μM (*21*). The binding site on the SH3 surface is made up of three pockets, of which two are sufficiently large to

† Financial support was obtained from the Schweizerischer Nationalfonds and the ETH Zürich through the National Center of Competence in Research (NCCR) Structural Biology.

* To whom correspondence should be addressed. Phone: +41 (0)1 633 2473. Fax: +41 (0)1 633 1151. E-mail: wuthrich@mol.biol.ethz.ch.

[1] Abbreviations: NMR, nuclear magnetic resonance; CD, circular dichroism; Grb2, growth factor receptor-bound protein 2; SH3, Src homology domain 3; Grb2_cSH3, carboxy-terminal SH3 domain of murine Grb2; PrP, prion protein; mPrP, murine prion protein; mPrP-(90−231), recombinant mouse prion protein containing residues 90−231; mPrP(90−231)[P101L], variant of mPrP(90−231) with proline 101 replaced by leucine; mPrP(90−231)[P104L], variant of mPrP(90−231) with proline 104 replaced by leucine; PrP^{C}, cellular isoform of PrP; PrP^{Sc}, scrapie isoform of PrP; *Prnp*, gene coding for PrP; GSS, Gerstmann−Sträussler−Scheinker sydrome; TSE, transmissible spongiform encephalopathies.

10.1021/bi0494828 CCC: $27.50
Published on Web 07/24/2004

Mouse	^{99}N	*K*	**P**	S	*K*	**P**	*K*	T	N	L	*K*	H
Chicken	^{105}Q	*K*	**P**	W	*K*	**P**	**P**	*K*	T	**N**	F	*K*
Turtle	^{119}Q	*K*	**P**	W	*K*	**P**	D	*K*	**P**	*K*	T	N
Xenopus	^{69}N	*K*	Q	W	*K*	**P**	**P**	*K*	S	*K*	T	N
Fugu	^{278}Y	*K*	**P**	*K*	S	**P**	S	T	A	*K*	*K*	A

FIGURE 1: Amino acid sequence alignment for the presently identified SH3-binding motif of prion proteins from different species. Amino acid residues 99−110 of mPrP, which correspond to residues 100−111 of hPrP, are representative of all mammalian PrPs (*10*, *11*). Prolines are shown in bold, positively charged amino acids are in italics, and negatively charged residues are underlined. The sequence number of the first residue is indicated.

accommodate a prolyl residue and the third one can accommodate a positively charged residue at the end of the binding ligand (*22*). SH3 domains are also known to interact with GPI-anchored proteins (*23*). SH3 domains target their partner proteins to the cell membrane or other cellular compartments, activate or inactivate their function, or regulate their local concentration (*21*).

Mammalian PrP sequences include a highly conserved potential SH3-binding motif comprising residues 101−104 (Figure 1) (the murine prion protein numbering is used throughout this paper). In this study we wanted to further investigate, with physicochemical and structural biology techniques, whether Grb2_cSH3 could really act as a physiologically relevant partner for PrP^C and, thus, more firmly establish a role for PrP^C in signal transduction. Added interest in this study comes from the observations that the PxxP motif of residues 101−104 in mPrP corresponds to polypeptide segment 102−105 in hPrP, of which the two variants P102L and P105L have been related to increased susceptibility to the Gerstmann−Sträussler−Scheinker syndrome (*24*, *25*). It has also been shown by immunofluorescence microscopy that Grb2 and PrP^C colocalize on the cell surface during *Brucella abortus* swimming internalization, which itself is promoted by PrP^C (*26*). A potential physiological role of the PrP^C−Grb2 interaction is also indicated by recent investigations of the localization of PrP^C in living cells. Immunomicroscopy pictures revealed that, in the hippocampus, the neocortex, and the thalamus, PrP^C is predominantly located in the cytosol (*27*). These new studies also indicate that, in contrast to earlier reports (*28*), cytosolic PrP does not seem to be neurotoxic in these cells (*27*).

EXPERIMENTAL PROCEDURES

Cloning, Expression, and Purification of the Proteins. The protein fragments mPrP(90−231), mPrP(90−231)[P101L], mPrP(90−231)[P104L], mPrP(121−231), and Grb2_cSH3 were cloned into the vector pRSETA, which contains a His_6 tag and a thrombin cleavage site between the His_6 tag and the protein fragment. The proteins were expressed in *Escherichia coli* BL21 cells.

The PrP fragments were purified according to Zahn et al. (*3*, *29*). Modifications of the previously published protocol were that thrombin was removed with *p*-aminobenzamidine Celite (Sigma, A-5825), that an additional centrifugation step was used to remove the Celite, and that no ion-exchange chromatography step was used. The protein solutions were lyophilized, redissolved in water, and dialyzed in a buffer containing 50 mM sodium phosphate at pH = 7.0, 20 mM NaCl, and 0.05% sodium azide (PB buffer) to give a final protein concentration of 3 mM.

Grb2_cSH3 was purified in the same way as the PrP fragments, except that 0.1 mM DTT was added to the eluted protein to keep the free cysteine in the reduced state. An additional gel filtration chromatography step (HiLoad 26/60 Superdex, Pharmacia Biotech) was used to remove residual impurities of Grb2_cSH3 dimers and other proteins. The Grb2_cSH3 solution was lyophilized, redissolved in water, and dialyzed against PB buffer to give a final protein concentration of 5 mM.

^{1}H NMR spectroscopy was used to check that the proteins were properly folded. mPrP(90−231) was also prepared in uniformly ^{15}N-labeled form. The protein concentrations were determined by absorbance spectroscopy according to Gill and von Hippel (*30*).

NMR Experiments. Steady-state ^{15}N{^{1}H}-nuclear Overhauser enhancements (NOEs) were measured according to Dayie and Wagner (*31*) on a Bruker DRX500 spectrometer equipped with a cryoprobe, using a saturation period of 4 s. The NMR samples contained 1 mM mPrP(90−231) and either 0, 0.4, 0.8, or 1.0 mM Grb2_cSH3 in PB buffer containing 5% D_2O.

Chemical shift changes in ^{15}N-labeled mPrP(90−231) upon addition of 1 equiv of Grb2_cSH3, $\Delta\delta$, were measured using [^{15}N,^{1}H]-COSY spectra recorded on a Bruker DRX500 spectrometer equipped with a cryoprobe. In three different experiments, the mPrP(90−231) concentration in the NMR samples was 0.02, 0.05, or 1 mM in PB buffer containing 5% D_2O.

The NMR data were processed with the program PROSA (*32*), and the resulting spectra were analyzed with the program XEASY (*33*).

Fluorescence Spectroscopy. Due to the proximity of tryptophans to the binding sites in both proteins (Grb2_cSH3, W197 and W198; mPrP(90−231), W99), fluorescence spectroscopy could be used to determine the binding constant K_D for the complex between Grb2_cSH3 and various mouse PrP fragments (Figures 3 and 4). All fluorescence spectra were recorded at 25 °C on a Hitachi F-4500 fluorescence spectrophotometer in a 10 × 2 mm quartz cuvette. The samples were excited at 290 nm, and measurements were taken at 350 nm in intervals of 0.2 s and averaged over 10 s. The samples contained either 5 μM mPrP(90−231), mPrP(90−231)[P101L], or mPrP(90−231)[P104L] and from 0 to 20 μM Grb2_cSH3. For a more precise determination of the binding constant K_D for the interaction of mPrP(90−231) with Grb2_cSH3, a second set of experiments was started with a solution of 5 μM Grb2_cSH3, and from 0 to 10 μM mPrP(90−231) was added in a stepwise fashion.

All fluorescence experiments were performed in PB buffer. Calibration curves for the fluorescence signal intensity of all proteins at 350 nm were recorded and subtracted from the data used to calculate the binding constants K_D. After initial measurements at 5 μM concentration of one protein, the second protein was added in small steps to give changes in the final concentration either of 0.5 μM [addition of mPrP(90−231) to Grb2_cSH3] or of 2.5 μM [addition of Grb2_cSH3 to mPrP(90−231), mPrP(90−231)[P101L], or mPrP(90−231)[P104L]]. The results were corrected for the small volume changes and the intrinsic filter effect. The change of the fluorescence intensity, which is due to the

change in hydrophobicity of the environment of the tryptophans (*34*), was plotted against the amount of the titrated protein. The program ORIGIN was used to fit the K_D curves and determine the binding constants via the equation:

$$\Delta I = \frac{I_\infty[\text{protB}]}{K_D + [\text{protB}]} \quad (1)$$

where [protB] is the concentration of the added protein, ΔI the measured fluorescence change, I_∞ the maximum fluorescence change at full complex formation, and K_D the binding constant.

Circular Dichroism Spectroscopy. Far-UV circular dichroism (CD) spectra were measured at 25 °C on a Jasco 810 CD spectropolarimeter in 0.1 cm quartz cuvettes. Twelve traces were accumulated and averaged, the data were corrected for the effect from the buffer, and the signal of Grb2_cSH3 was subtracted from the signal of the protein−protein complex. The samples contained 10 μM protein or protein−protein complex, 2.5 mM sodium phosphate at pH = 7.0, and 1 mM NaCl.

Molecular Modeling. The three-dimensional structure of the PrP^C−Grb2_cSH3 complex was modeled using the coordinates of the solution structure of Grb2_cSH3 [PDB entry 1GFC (*18*)] and of the ligand in the crystal structure of the Abl tyrosine kinase SH3 domain by Musacchio et al. [PDB entry 1ABO (*35*)] as a starting platform. The ligand from the latter reference was then remodeled with the program Sybyl 6.6 (Tripos) to represent the polypeptide fragment with the sequence of mPrP(100−109). This decapeptide was interactively positioned into the binding pocket of Grb2_cSH3, with its sequence running from left to right ["class II ligand" (*21*)]. (The final result from this calculation is shown in Figure 6.) The resulting structure of the complex between Grb2_cSH3 and mPrP(100−109) was then optimized with the subroutine FlexiDock implemented in the program SYBYL 6.6. All side chains of Grb2_cSH3 and the complete structure of mPrP(100−109), including the electrostatic charges, were kept flexible during this two-step docking procedure. The resulting complex was energy-minimized with the program Sybyl 6.6, using the Amber force field. The procedure was repeated with mPrP(100−109) oriented in the opposite direction in the binding pocket ["class I ligand" (*21*)].

RESULTS

Identification of the Sequence Location of the SH3 Binding Site on PrP^C by Circular Dichroism (CD) Spectroscopy. After addition of 1 equiv of Grb2_cSH3, the CD spectrum of mPrP(90−231) shows an increase of about 15% in the molar ellipticity of the minima near 210 and 222 nm (Figure 2A). This change in the signal intensities is indicative of a transition of a random coil polypeptide segment to a helical conformation when Grb2_cSH3 binds to PrP^C. We attribute this transition to mPrP(90−231) for the following two reasons. First, there is evidence that SH3 domains do not undergo extensive conformational changes upon ligand binding (*36*). Second, polypeptide segment 90−125 in mPrP(90−231) is known to be flexibly unstructured in the absence of interactions with other proteins (*7*).

In a first-level attempt to more precisely locate the interaction site, mPrP(121−231) was measured in the absence and presence of Grb2_cSH3. No change in the CD spectrum of mPrP(121−231) was observed (Figure 2B). Comparison of the data in the Figure 2A,B thus indicates that the interaction site between PrP^C and Grb2_cSH3 is between residues 90 and 120 in the flexible N-terminal tail of mPrP(90−231).

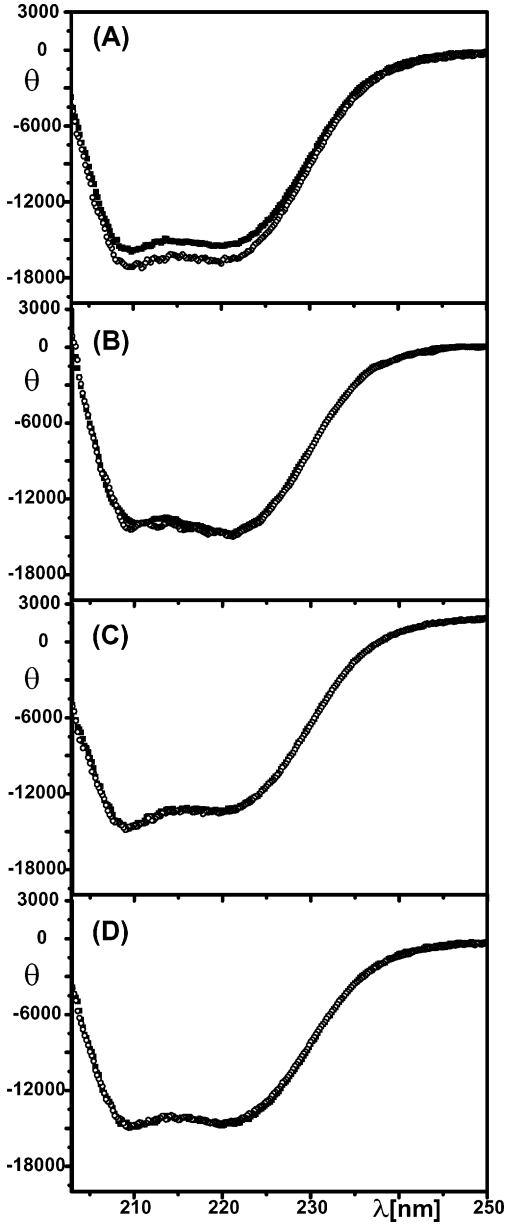

FIGURE 2: Circular dichroism spectra of 10 μM solutions of four different PrP fragments in the absence (black squares) and presence (open circles) of 10 μM Grb2_cSH3: (A) mPrP(90−231); (B) mPrP(121−231); (C) mPrP(90−231)[P104L]; (D) mPrP(90−231)-[P101L]. The molar ellipticity, Θ (in deg·cm^2·dmol^{-1}), is plotted versus the wavelength (in nm).

Residues 101−104 of mPrP form a PxxP motif, which is known to be an SH3-binding site (*21*, *22*). As a second-level attempt to locate the SH3-binding site, CD measurements were also performed with mPrP(90−231)[P101L] and mPrP(90−231)[P104L]. Neither of these two mPrP variants showed a significant change in the CD spectrum upon addition of Grb2_cSH3 (Figure 2C,D). Comparison with the data of Figure 2A then implies that the interaction between mPrP(90−231) and Grb2_cSH3 involves quite specifically the region of residues 101−104 and that this interaction is

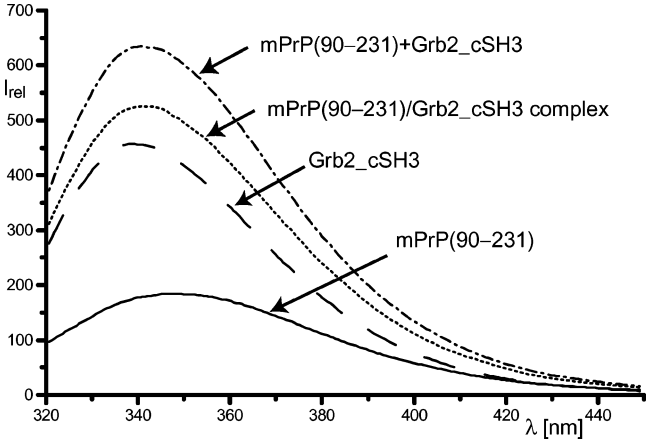

FIGURE 3: Fluorescence intensity, I_{rel}, from 320 to 450 nm of mPrP(90−231) (solid line), Grb2_cSH3 (broken line), and the complex of mPrP(90−231) and Grb2_cSH3 (dotted line). The dashed−dotted line is the sum of the fluorescence intensities of mPrP(90−231) and Grb2_cSH3.

abolished by either of the amino acid substitutions P101L and P104L.

Conservation of the SH3 Binding Site in the Known Prnp Genes. Comparison of the known vertebrate *Prnp* genes reveals a conserved SH3-binding motif, which slightly varies only in the *Xenopus lavis Prnp* gene (Figure 1). It is also quite striking that there are four lysines in the dodecapeptide segment corresponding to residues 99−110 in mPrP (Figure 1). The position of the lysines varies only slightly among the different species, and a strongly positive overall charge of this polypeptide stretch seems to be conserved within all known PrPs.

Determination of the Binding Affinity of Wild-Type and Variant PrP^C for Grb_cSH3. There are three tryptophans near the presumed interaction site of mPrP(90−231) and Grb2_cSH3, i.e., W197 and W198 of Grb2_cSH3 and W99 of mPrP(90−231). It was therefore not unexpected that the fluorescence signal reflects the binding of mPrP(90−231) and Grb2_cSH3 (Figure 3) and could thus be used to investigate the binding affinity between the two proteins.

The combined fluorescence signal of mPrP and Grb2_cSH3 was partially quenched when Grb2_cSH3 was added stepwise to mPrP(90−231). These data could be fitted with a binding constant K_D = 10.6 (±5.5) μM (Figure 4A). In contrast, the same experiment with mPrP(90−231)[P101L] showed only a small increase in fluorescence intensity upon addition of Grb2_cSH3 (Figure 4B), indicating an upper limit for the binding affinity between mPrP(90−231)[P101L] and Grb2_cSH3, with $K_D \gtrsim 60$ μM. An identical experiment with mPrP(90−231)[P104L] showed no significant change in the fluorescence signal upon addition of Grb2_cSH3 (Figure 4B), indicating $K_D \gtrsim 150$ μM as an upper limit for the binding affinity.

To verify the value for the binding affinity of mPrP(90−231) for Grb2_cSH3 given in Figure 4A, the fluorescence signal change was also recorded during stepwise addition of mPrP(90−231) to Grb2_cSH3. By recording a larger number of data points, a significantly more precise determination of the binding affinity was achieved, with K_D = 5.5 (±0.5) μM (Figure 4C).

Structural and Dynamic Aspects of the Grb2_cSH3−mPrP(90−231) Interactions from NMR Spectroscopy. Upon

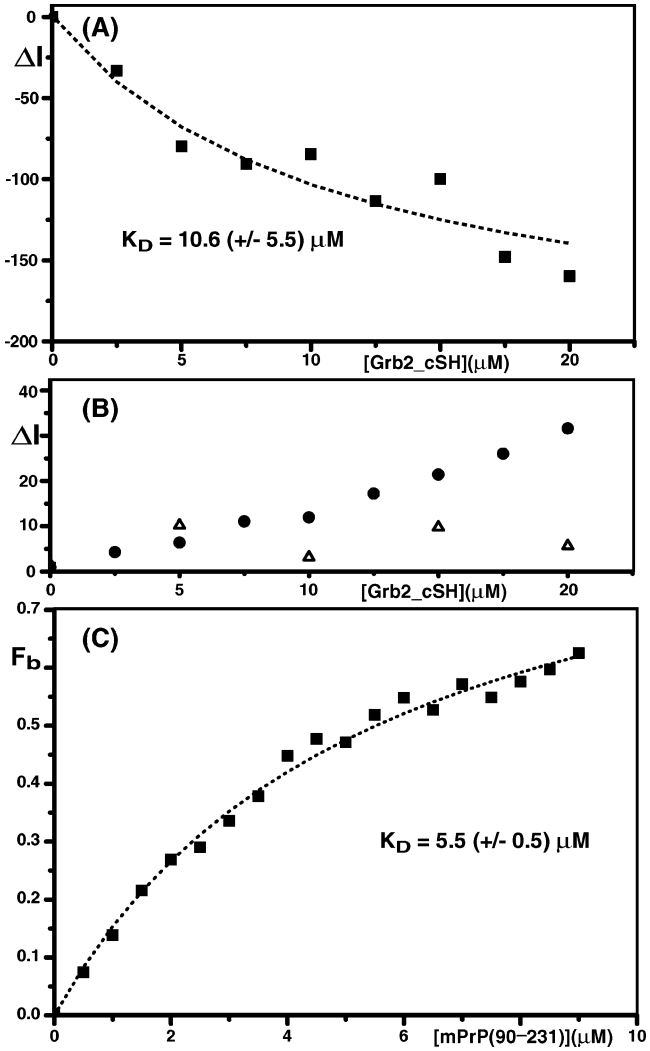

FIGURE 4: (A) Fluorescence titration curves manifesting the binding of Grb2_cSH3 with mPrP(90−231) (filled squares). Plotted is the change in fluorescence intensity, ΔI, versus the concentration of Grb2_cSH3 added to a solution of mPrP(90−231). The prion protein concentrations at the start and the end of the titration were 5.00 and 4.93 μM, respectively. (B) Same experiment as in (A), whereby Grb2_cSH3 was added to mPrP(90−231)[P101L] (filled circles) and mPrP(90−231)[P104L] (open triangles). (C) Reverse fluorescence titration used for verification of the binding constant, K_D, for mPrP(90−231) interacting with Grb2_cSH3 [see (A)]. Plotted is the fraction of complexed Grb2_cSH3, F_b, versus the concentration of mPrP(90−231) added to a Grb2_cSH3 solution. The Grb2_cSH3 concentrations at the start and at the end of the titration were 5.00 and 4.95 μM, respectively.

stepwise addition of unlabeled Grb2_cSH3, the [^{15}N,^{1}H]-COSY spectra of uniformly ^{15}N-labeled mPrP(90−231) showed a monotonic increase of chemical shift changes, and no splitting of resonances was observed. This demonstrates that the mPrP(90−231) exchange between the free form and the PrP^C−Grb2_cSH3 complex is rapid on the chemical shift time scale; i.e., it has a value of $k_{off} \gtrsim 1000$ s^{-1}.

The flexibility of the polypeptide chain in PrP^C was assessed on the basis of ^{15}N{^{1}H}-NOE measurements. The ^{15}N{^{1}H}-NOE data are complete except for residues 168, 170−173, and 175, for which the amide−proton resonances are not detectable presumably due to conformational exchange (*2*), and of course for all proline residues. Overall, the ^{15}N{^{1}H}-NOEs manifest the structured C-terminal domain of residues 128−231, with somewhat increased flex-

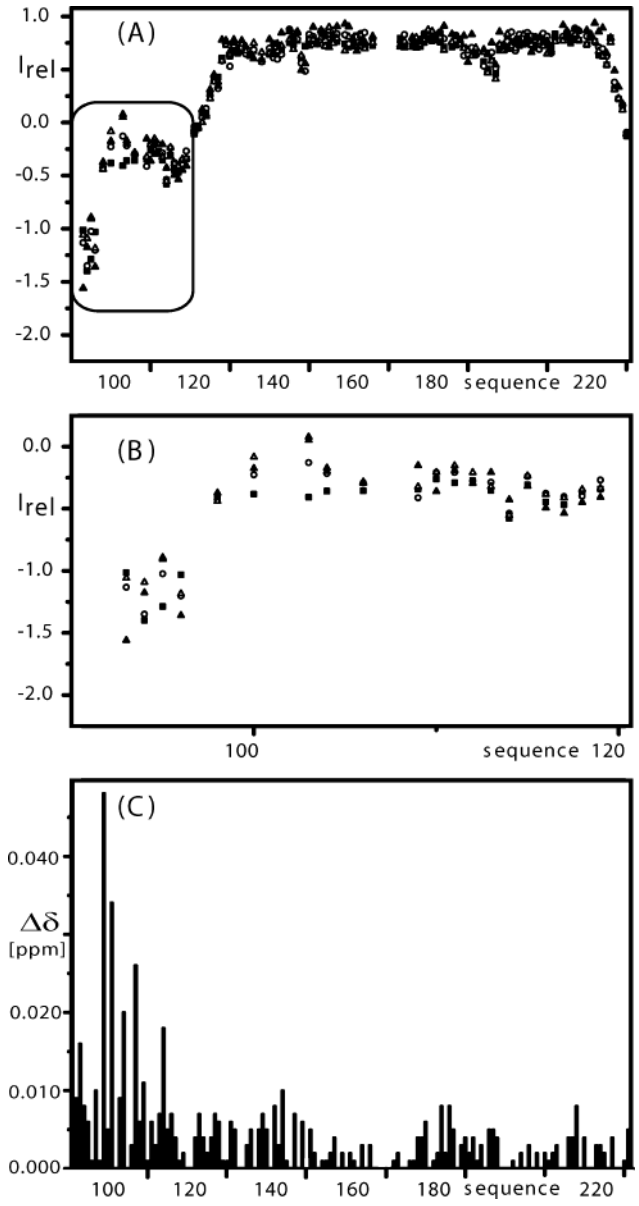

FIGURE 5: NMR studies of the mPrP(90−231)/Grb2_cSH3 interaction. (A) Heteronuclear $^{15}N\{^1H\}$-NOE intensities of uniformly ^{15}N-labeled mPrP(90−231) in the absence of Grb2_cSH3 (black squares) and after addition of 0.4 equiv (open circles), 0.8 equiv (open triangles), and 1.0 equiv (black triangles) of unlabeled Grb2_cSH3. (B) Expanded plot of the data in (A) for residues 90−120. In the experiments in (A) and (B) the mPrP(90−231) concentration was 1.0 mM in 50 mM phosphate at pH 7.0 containing 20 mM NaCl, 0.05% NaN_3, and 5% D_2O. (C) Chemical shift changes, $\Delta\delta$ (in ppm), of the backbone amide protons of mPrP(90−231) upon addition of 1.0 equiv of Grb2_cSH3. The mPrP(90−231) concentration was 20 μM in the same buffer as used for (A) and (B). Both the $^{15}N\{^1H\}$-NOE and the amide proton chemical shift data for mPrP(90−231) are complete, except for residues 168, 170−173, and 175, for which the amide−proton resonances are undetectable (*2*).

ibility of the polypeptide chain toward the C-terminus, and the presence of a flexibly disordered N-terminal tail of residues 90−128. Along this tail, the flexibility increases from its attachment point to the globular domain toward the N-terminus, except that locally restricted flexibility around residues 99−115 was detected (Figure 5A,B). This observation is indicative of residual structure for this segment within the otherwise flexibly disordered tail. Upon the stepwise addition of Grb2_cSH3, the $^{15}N\{^1H\}$-NOEs show evidence of reduced flexibility for fragment 100−105 (Figure 5A,B), since the intensity of the $^{15}N\{^1H\}$-NOEs for these residues increases monotonically with the increase of the Grb2_cSH3 concentration (Figure 5B).

Amide−proton chemical shift changes upon addition of 1 equiv of unlabeled Grb2_cSH3 were measured in [^{15}N,^1H]-COSY spectra of 0.02 mM ^{15}N-labeled mPrP(90−231) (Figure 5C). These data confirm the implication from CD spectroscopy (Figure 2) and the $^{15}N\{^1H\}$-NOE data (Figure 5A,B) that the primary interaction site of mPrP(90−231) with Grb2_cSH3 involves mPrP residues 100−115, since significant chemical shift changes are seen only for residues in this polypeptide segment. We repeated the experiment of Figure 5C at higher protein concentrations (data not shown). Even at 1 mM mPrP(90−231) the selectivity of the interaction seen in Figure 5C was no longer apparent, since comparable values of $\Delta\delta$ were obtained for selected residues in the regions 112−150 and 176−185. At higher protein concentrations the amide−proton chemical shift changes thus appear to manifest multiple lower affinity interaction sites on the PrP^C surface, in addition to the primary contacts in segment 100−115. This would appear to be compatible with previous reports on nonspecific protein contacts with other SH3 domains (*37*).

Molecular Modeling of the Complex of Grb2_cSH3 and mPrP(101−110). In an attempt to rationalize the protein−protein interaction data of Figures 2−5 on the molecular structure level, this section supplements the experimental studies with modeling of the intermolecular interaction. The starting platform for this part of the project was the previous observation in several crystal and solution structures that SH3 domains bind their proline-rich ligands in a polyproline II (PPII) conformation (*22*). Since the solution structure of Grb2_cSH3 (*18*) does not show the bound ligand, a decapeptide with the sequence of mPrP(100−109) (Figure 1) was generated in the PPII conformation and then docked into the binding pocket of Grb2_cSH3. In the resulting complex of mPrP(100−109) and Grb2_cSH3 (Figure 6), the binding pocket on Grb2_cSH3 is highly negatively charged (Figure 6B), whereas mPrP(100−109) is positively charged (Figure 6C,D). The two protein surfaces thus bear strikingly complementary electrostatic charges (Figure 6B,D), with mPrP(100−109) having four lysines and no aspartates or glutamates among the 10 amino acids (Figure 1). There is thus a strong indication also from this modeling approach that electrostatic forces are responsible for the high affinity of the two proteins toward each other, when compared with other known SH3−ligand interactions (*21*).

DISCUSSION

Experiments with yeast two-hybrid systems and immunoprecipitation had previously shown that PrP^C and Grb2 interact in vitro (*14*), and immunofluorescence microscopy showed that PrP^C and Grb2 colocalize in vivo (*26*, *27*). The present paper supplements these earlier observations with physicochemical data on this protein−protein recognition process in vitro and with molecular modeling of the structure of the PrP^C−Grb2 complex.

Thermodynamics and Kinetics of the PrP^C−Grb2 Complex Formation. Overall, the data obtained with NMR, CD, and

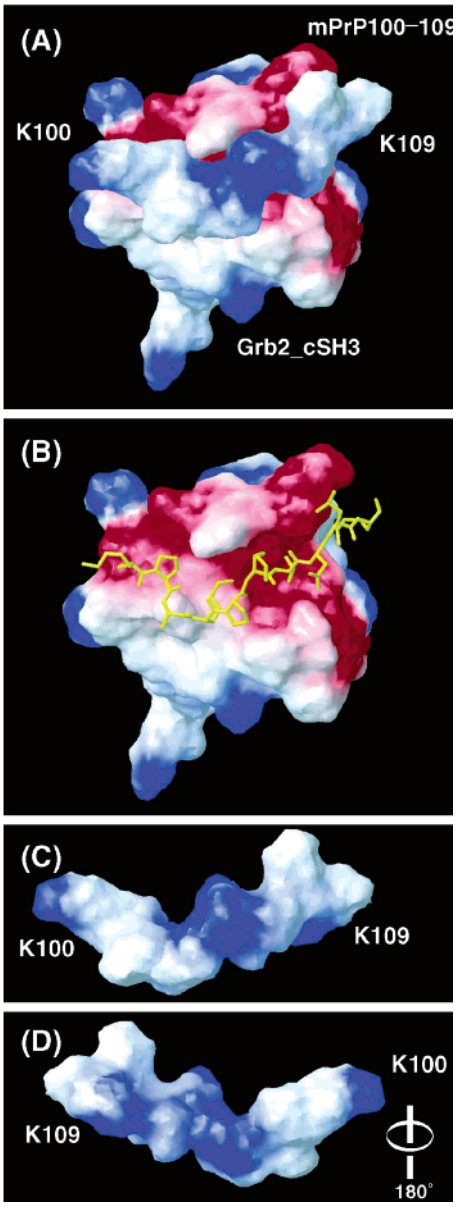

FIGURE 6: Molecular model of the complex formed by Grb2_cSH3 and the mPrP fragment with residues 100−109. In the surface representations, negative charges are shown in red and positive ones in blue. (A) Surface representation of Grb2_cSH3 with mPrP(100−109) in the binding pocket. (B) Same as (A), with mPrP(100−109) shown as a yellow stick drawing. (C) and (D) show mPrP(100−109) in the bound polyproline II conformation: (C) same orientation as in (A); (D) after rotation by 180° with respect to (C) around the axis indicated, showing the surface that is in contact with Grb2_cSH3.

fluorescence spectroscopy (Figures 2−5) convincingly show that the Grb2_cSH3 interaction involves the flexible tail of residues 90−120 in mPrP(90−231) and then narrows down the identification of the binding site to the intact -Pro101-Ser-Lys-Pro104- segment (Figure 1). The fluorescence data of Figure 4C also reveal that the affinity of mPrP(90−231) for Grb2_cSH3 is near the upper end of the range of complex stabilities reported for other SH3-binding ligands (*21*). NMR experiments further indicated that the complex formed between mPrP(90−231) and Grb2_cSH3 is short-lived on the chemical shift time scale, with a lifetime shorter than about 10^{-3} s. Finally, $^{15}N\{^{1}H\}$-NOE data provide additional support for the identification by the CD experiments of the polypeptide segment of residues 100−105 of mPrP(90−231) as a specific binding site (Figure 5A,B).

Evolutionary Considerations. In view of the molecular model of Figure 6, the evolutionary conservation of the SH3-binding site in PrP (Figure 1) gains added interest. All vertebrate species retain the PxxP motif, with the sole exception of *X. laevis* (Figure 1). Furthermore, birds and reptiles have even an additional proline in the binding region. In *X. laevis* the loss of Pro in position 71 (Figure 1) might be compensated with the addition of a second proline in position 75, which is next to the binding site. In addition to the conservation of the two prolines, the high conservation of lysines is striking. In all species, the dodecapeptide segments in Figure 1 contain four lysines, the lysine in the mPrP position 100 is strictly conserved, and all species contain one lysine in the dipeptide corresponding to mPrP-(102−103). The turtle prion protein is the only known vertebrate to have a negatively charged amino acid in the segment corresponding to mPrP(99−110), but it nonetheless maintains a positive overall charge for this segment.

Assuming that in addition to the positive charge of the mPrP(100−109) segment, the negative surface of Grb2_cSH3 is also conserved in the different species, the PrP^{C}−Grb2_cSH3 interaction driven by the presence of a PPII conformation of PrP(100−104) and the opposite electrostatic charges might relate to an early acquired function of PrP^{C}. The interaction of Grb2_cSH3 and PrP^{C} is of physiologically relevant strength (Figure 4C), and it involves a molecular region of PrP^{C} that is sterically inaccessible in PrP^{Sc}. This all would be expected in connection with a role of PrP^{C} in signal transduction, and it is tempting to speculate that this function might be lacking in patients with prion diseases.

Relations with GSS-Related Mutations in the Human Prion Proteins. The protein−protein interaction between PrP^{C} and Grb2 gains further interest because one of the most thoroughly investigated mutations of the PrP gene relating to familial TSEs in humans, P102L (P101L in mPrP), lies within the observed PrP^{C} binding site to Grb2_cSH3 (*24*, *25*). There have been several reports that a second mutation in the PxxP binding motif, P105L (P104L in mPrP), has been found in patients presenting with GSS (*38*). The fact that two mutations relating to the Gerstmann−Sträussler−Scheinker syndrome lie within the Grb2 binding site of PrP^{C} and that they abolish Grb2 binding thus implies that the Grb2−PrP^{C} interaction or, more precisely, the loss thereof might have a key role in the pathology of GSS patients.

Possible Relations with Other Physiological Processes. A recent publication presented evidence that Grb2 colocalizes with PrP^{C} during the swimming internalization of *B. abortus* with its host cell (*26*). Considering that PrP^{C} is needed for the *B. abortus* internalization into macrophages, it has been suggested that the bacterium hijacks an existing signal transduction pathway (*26*). The interaction between PrP^{C} and Grb2 during swimming internalization of *B. abortus* could thus, for example, lead to cytoskeletal rearrangement and generalized membrane ruffling (*26*), perhaps via the Grb2−WASP interaction along the way of the internalization of the bacterium (*39*).

ACKNOWLEDGMENT

We thank Prof. D. Kohda for providing the chemical shift lists for Grb2_cSH3, Prof. H. M. Schätzl and Dr. C.

Spielhaupter for the Grb2 gene, and Dr. H. Eberl for the constructs of the two variant mouse PrP genes.

REFERENCES

1. Weissmann, C., Enari, M., Klohn, P. C., Rossi, D., and Flechsig, E. (2002) Transmission of prions, *Proc. Natl. Acad. Sci. U.S.A. 99*, 16378−16783.
2. Riek, R., Hornemann, S., Wider, G., Billeter, M., Glockshuber, R., and Wüthrich, K. (1996) NMR structure of the mouse prion protein domain PrP(121−321), *Nature 382*, 180−182.
3. Zahn, R., Liu, A., Lührs, T., Riek, R., von Schroetter, C., López García, F., Billeter, M., Calzolai, L., Wider, G., and Wüthrich, K. (2000) NMR solution structure of the human prion protein, *Proc. Natl. Acad. Sci. U.S.A. 97*, 145−150.
4. López García, F., Zahn, R., Riek, R., and Wüthrich, K. (2000) NMR structure of the bovine prion protein, *Proc. Natl. Acad. Sci. U.S.A. 97*, 8334−8339.
5. James, T. L., Liu, H., Ulyanov, N. B., Farr-Jones, S., Zhang, H., Donne, D. G., Kaneko, K., Groth, D., Mehlhorn, I., Prusiner, S. B., and Cohen, F. E. (1997) Solution structure of a 142-residue recombinant prion protein corresponding to the infectious fragment of the scrapie isoform, *Proc. Natl. Acad. Sci. U.S.A. 94*, 10086−10091.
6. Wille, H., Michelitsch, M. D., Guenebaut, V., Supattapone, S., Serban, A., Cohen, F. E., Agard, D. A., and Prusiner, S. B. (2002) Structural studies of the scrapie prion protein by electron crystallography, *Proc. Natl. Acad. Sci. U.S.A. 99*, 3563−3568.
7. Riek, R., Hornemann, S., Wider, G., Glockshuber, R., and Wüthrich, K. (1997) NMR characterization of the full-length recombinant murine prion protein, mPrP(23−231), *FEBS Lett. 413*, 282−288.
8. Downing, D. T., and Lazo, N. D. (1999) Molecular modelling indicates that the pathological conformations of prion proteins might be beta-helical, *Biochem. J. 343*, 453−460.
9. Bueler, H., Aguzzi, A., Sailer, A., Greiner, R. A., Autenried, P., Aguet, M., and Weissmann, C. (1993) Mice devoid of PrP are resistant to scrapie, *Cell 73*, 1339−1347.
10. Van Rheede, T., Smolenaars, M. M., Madsen, O., and De Jong, W. W. (2003) Molecular evolution of the mammalian prion protein, *Mol. Biol. Evol. 20*, 111−121.
11. Wopfner, F., Weidenhofer, G., Schneider, R., von Brunn, A., Gilch, S., Schwarz, T. F., Werner, T., and Schätzl, H. M. (1999) Analysis of 27 mammalian and 9 avian PrPs reveals high conservation of flexible regions of the prion protein, *J. Mol. Biol. 289*, 1163−1178.
12. Mouillet-Richard, S., Laurendeau, I., Vidaud, M., Kellermann, O., and Laplanche, J. L. (1999) Prion protein and neuronal differentiation: quantitative analysis of Prnp gene expression in a murine inducible neuroectodermal progenitor, *Microbes Infect. 1*, 969−976.
13. Mouillet-Richard, S., Ermonval, M., Chebassier, C., Laplanche, J. L., Lehmann, S., Launay, J. M., and Kellermann, O. (2000) Signal transduction through prion protein, *Science 289*, 1925−1928.
14. Spielhaupter, C., and Schätzl, H. M. (2001) PrP^C directly interacts with proteins involved in signaling pathways, *J. Biol. Chem. 276*, 44604−44612.
15. Lowenstein, E. J., Daly, R. J., Batzer, A. G., Li, W., Margolis, B., Lammers, R., Ullrich, A., Skolnik, E. Y., Bar-Sagi, D., and Schlessinger, J. (1992) The SH2 and SH3 domain-containing protein GRB2 links receptor tyrosine kinases to ras signaling, *Cell 70*, 431−442.
16. Cheng, A. M., Saxton, T. M., Sakai, R., Kulkarni, S., Mbamalu, G., Vogel, W., Tortorice, C. G., Cardiff, R. D., Cross, J. C., Muller, W. J., and Pawson, T. (1998) Mammalian Grb2 regulates multiple steps in embryonic development and malignant transformation, *Cell 95*, 793−803.
17. Buday, L. (1999) Membrane-targeting of signaling molecules by SH2/SH3 domain-containing adaptor proteins, *Biochim. Biophys. Acta 1422*, 187−204.
18. Kohda, D., Terasawa, H., Ichikawa, S., Ogura, K., Hatanaka, H., Mandiyan, V., Ullrich, A., Schlessinger, J., and Inagaki, F. (1994) Solution structure and ligand-binding site of the carboxy-terminal SH3 domain of GRB2, *Structure 2*, 1029−1040.
19. Yuzawa, S., Yokochi, M., Hatanaka, H., Ogura, K., Kataoka, M., Miura, K., Mandiyan, V., Schlessinger, J., and Inagaki, F. (2001) Solution structure of Grb2 reveals extensive flexibility necessary for target recognition, *J. Mol. Biol. 306*, 527−537.
20. Wittekind, M., Mapelli, C., Farmer, B. T., II, Suen, K. L., Goldfarb, V., Tsao, J., Lavoie, T., Barbacid, M., Meyers, C. A., and Mueller, L. (1994) Orientation of peptide fragments from Sos proteins bound to the N-terminal SH3 domain of Grb2 determined by NMR spectroscopy, *Biochemistry 33*, 13531−13539.
21. Mayer, B. J. (2001) SH3 domains: complexity in moderation, *J. Cell. Sci. 114*, 1253−1263.
22. Kay, B. K., Williamson, M. P., and Sudol, M. (2000) The importance of being proline: the interaction of proline-rich motifs in signaling proteins with their cognate domains, *FASEB J. 14*, 231−241.
23. Thomas, S. M., and Brugge, J. S. (1997) Cellular functions regulated by Src family kinases, *Annu. Rev. Cell Dev. Biol. 13*, 513−609.
24. Telling, G. C., Haga, T., Torchia, M., Tremblay, P., DeArmond, S. J., and Prusiner, S. B. (1996) Interactions between wild-type and mutant prion proteins modulate neurodegeneration in transgenic mice, *Genes Dev. 10*, 1736−1750.
25. Manson, J. C., Jamieson, E., Baybutt, H., Tuzi, N. L., Barron, R., McConnell, I., Somerville, R., Ironside, J., Will, R., Sy, M. S., Melton, D. W., Hope, J., and Bostock, C. (1999) A single amino acid alteration (101L) introduced into murine PrP dramatically alters incubation time of transmissible spongiform encephalopathy, *EMBO J. 18*, 6855−6864.
26. Watarai, M., Kim, S., Erdenebaatar, J., Makino, S., Horiuchi, M., Shirahata, T., Sakaguchi, S., and Katamine, S. (2003) Cellular prion protein promotes *Brucella* infection into macrophages, *J. Exp. Med. 198*, 5−17.
27. Mironov, A., Jr., Latawiec, D., Wille, H., Bouzamondo-Bernstein, E., Legname, G., Williamson, R. A., Burton, D., DeArmond, S. J., Prusiner, S. B., and Peters, P. J. (2003) Cytosolic prion protein in neurons, *J. Neurosci. 23*, 7183−7193.
28. Ma, J., Wollmann, R., and Lindquist, S. (2002) Neurotoxicity and neurodegeneration when PrP accumulates in the cytosol, *Science 298*, 1781−1785.
29. Zahn, R., von Schroetter, C., and Wüthrich, K. (1997) Human prion proteins expressed in *Escherichia coli* and purified by high-affinity column refolding, *FEBS Lett. 417*, 400−404.
30. Gill, S. C., and von Hippel, P. H. (1989) Calculation of protein extinction coefficients from amino acid sequence data, *Anal. Biochem. 182*, 319−326.
31. Dayie, K. T., and Wagner, G. (1994) Relaxation-rate measurements for ^{15}N-^{1}H- groups with pulsed-field gradients and preservation of coherence pathways, *J. Magn. Reson. A 111*, 121−126.
32. Güntert, P., Dötsch, V., Wider, G., and Wüthrich, K. (1992) Processing of multidimensional NMR data with the new software Prosa, *J. Biomol. NMR 2*, 619−629.
33. Bartels, C., Xia, T. H., Billeter, M., Güntert, P., and Wüthrich, K. (1995) The program Xeasy for computer-supported NMR spectral-analysis of biological macromolecules, *J. Biomol. NMR 6*, 1−10.
34. Creighton, T. E. (1993) *Proteins: structures and molecular properties*, 2nd ed., W. H. Freeman, New York.
35. Musacchio, A., Saraste, M., and Wilmanns, M. (1994) High-resolution crystal structures of tyrosine kinase SH3 domains complexed with proline-rich peptides, *Nat. Struct. Biol. 1*, 546−551.
36. Feng, S., Chen, J. K., Yu, H., Simon, J. A., and Schreiber, S. L. (1994) Two binding orientations for peptides to the Src SH domain: Development of a general model for SH3-ligand interaction, *Science 266*, 1241−1247.
37. Okoh, M. P., and Vihinen, M. (2002) Interaction between Btk TH and SH3 domain, *Biopolymers 63*, 325−334.
38. Kovacs, G. G., Trabattoni, G., Hainfellner, J. A., Ironside, J. W., Knight, R. S., and Budka, H. (2002) Mutations of the prion protein gene phenotypic spectrum, *J. Neurol. 249*, 1567−1582.
39. She, H. Y., Rockow, S., Tang, J., Nishimura, R., Skolnik, E. Y., Chen, M., Margolis, B., and Li, W. (1997) Wiskott-Aldrich syndrome protein is associated with the adapter protein Grb2 and the epidermal growth factor receptor in living cells, *Mol. Biol. Cell 8*, 1709−1721.

BI0494828